Hydrological characteristics of extreme floods in the Klaserie River, a headwater stream in southern Africa

Sean Murray Marr,* Anthony Michael Swemmer

SAEON Ndlovu Node, Kruger National Park, Phalaborwa, 1390 South Africa

ABSTRACT

Climate change models for southern Africa predict less frequent, but more intense, rainfall events, and an increased frequency of tropical cyclones. With their steep topography and small catchments, headwater streams generate large floods following intense rainfall events. Large flooding events in headwater streams are under studied in southern Africa. In this paper, we explore flooding in the upper Klaserie River, Limpopo River System, South Africa, to determine the flow distribution and flood frequency for the catchment. In addition, we determine the return level for a large, economically damaging, flood generated following the landfall of a sub-tropical depression in January 2012 and, attempt to identify rainfall patterns that resulted in similar floods. An annual hydrological cycle with summer maxima and winter minima for both rainfall and flow was identified. The flood frequency analysis demonstrated that the January 2012 flood had an estimated return level of 225 years. This flood had a peak flowrate exceeding 1200 m^3s^{-1} in a system with an average daily flowrate of 1 m^3s^{-1}. Regression tree analysis showed that a two-day rainfall in excess of 240 was a predictor for four of the five largest floods. A two-day rainfall in excess of 400 mm distinguished the January 2012 flood from other floods. Non-stationarity analyses for the flow and rainfall data and a SWAT hydrological model are recommend for the upper Klaserie River to evaluate climate and land cover changes, and their relationship to the magnitude of the 2012 flood. Our study demonstrates that South African river monitoring data can be used to detect and characterize major floods, despite deficiencies in these data. Continuation of these monitoring programs is vital for river health monitoring and the detection of trends in floods resulting from human activities and climate change.

Corresponding author: erubescens@gmail.com

Key words: flow duration curves, flood frequency, flood hydrograph, Pardé coefficient, peaks over threshold, regression tree.

Citation: Marr SM, Swemmer AM. Hydrological characteristics of extreme floods in the Klaserie River, a headwater stream in southern Africa. *J. Limnol. 2023;82:2102*.

Edited by: Diego Fontaneto, *National Research Council, Water Research Institute (CNR-IRSA), Verbania Pallanza, Italy*.

Conflict of interest: The authors have no relevant financial or non-financial interests to disclose.

Contributions: the authors contributed equally to the study conception and design, material preparation, data collection and analysis. The authors read and approved the final version of the manuscript and agreed to be accountable for all aspects of the work.

Received: 28 October 2022.
Accepted: 15 March 2022.

Publisher's note: all claims expressed in this article are solely those of the authors and do not necessarily represent those of their affiliated organizations, or those of the publisher, the editors and the reviewers. Any product that may be evaluated in this article or claim that may be made by its manufacturer is not guaranteed or endorsed by the publisher.

Licensee PAGEPress, Italy
J. Limnol., 2023; 82:2102
DOI: 10.4081/jlimnol.2023.2102

INTRODUCTION

Despite freshwater habitats constituting about 0.8% of the Earth's surface area, they contain disproportionally high concentrations of biodiversity in comparison to terrestrial systems (Balian *et al.*, 2008). However, freshwaters are among the most extensively altered ecosystems (Carpenter *et al.*, 2011) and, once disturbed, deteriorate faster than terrestrial systems (Millennium Ecosystem Assessment, 2005). Headwater streams contain many specialist species and are among the most sensitive of the freshwater ecosystems (Richardson, 2019). Changes in climate, land use, and forest cover all impact headwater streams and alter the biogeochemical cycles in their catchments (Yamashita *et al.*, 2011). Headwater streams are particularly susceptible to the destructive power of floods because they have small catchments, steep topography, and are influenced by minor changes in local conditions (Meyer *et al.*, 2007). Extreme floods in headwater streams alter biogeochemical cycles and can result in major changes in the composition and structure of aquatic biotic communities (Feeley *et al.*, 2012).

Floods are also the leading cause of natural disaster mortalities worldwide (Doocy *et al.*, 2013). Between 1980 and 2009, Doocy *et al.* (2013) estimated that almost 3 billion people had been effected by flooding, including more than 500 000 mortalities and about 360 000 injuries. In addition, the socio-economic impacts of floods can be substantial. While the impact of floods on property and infrastructure damage, including agricultural losses, are

obvious, the full impacts of floods also include health, interruption of public services, and foregone production (Allaire, 2018). As global climate change progresses, and rainfall regimes become more extreme (Brooks *et al.*, 2020; Fowler *et al.*, 2021), the frequency of moderate, large and extreme floods, *sensu* Nathan and Weinmann (2019), are increasing globally (Westra *et al.*, 2014; Fowler *et al.*, 2021; Slater *et al.*, 2021a). Climate change models for the semi-arid lowveld region of South Africa predict no change in annual precipitation, but less frequent and more intense rainfall events (de Wit and Stankiewicz, 2006). In addition, an increased frequency of cyclone-generated moderate and large floods in eastern southern Africa is predicted (Fitchett, 2018); systems that have caused the majority of the recent flooding events in the lowveld (Heritage *et al.*, 2019). While the ecological and hydrological impacts of recent floods have been documented for the largest rivers of the lowveld (Heritage *et al.*, 2015; 2019), impacts on headwater streams have not been explored.

Although high rainfall is the primary driver of floods in headwater streams, the extent and magnitude of floods can be influenced by temperature, evapotranspiration, topography, landscape gradient, type of soil, soil infiltration rate, soil saturation level, land drainage, land use, land-cover, and river channel alterations including water retention and flood control structures (Cronshey, 1986; Sitterson *et al.*, 2018; Ball and Babister, 2019; Davie and Quinn, 2019). Small floods and flow variability are essential for the maintenance of channel geomorphology and resilience of biota to withstand the scouring flows of large floods (King *et al.*, 2003). In contrast, large floods reset, or fundamentally alter, the physical and chemical conditions underpinning the long-term development of biotic communities (Naiman *et al.*, 2008), potentially creating more heterogeneous and patchy riverscapes (Turner and Dale, 1998). The biotic and abiotic legacy of an large flood becomes the template upon which subsequent ecological processes build, and these events may, therefore, have a long-lasting influence on ecosystems and become catalysts for unexpected changes in ecosystems, including dramatic changes to aquatic and riparian communities (Turner and Dale, 1998; Parsons *et al.*, 2005; Milan *et al.*, 2018).

In January 2012, sub-tropical depression Dando made landfall resulting in 500 to 700 mm of rain falling in one day over the Klaserie River catchment, a tributary of the Olifants River, Limpopo River System, within the sub-tropical savanna lowveld region of South Africa. This resulted in a flood that caused substantial economic damage (Fitchett *et al.*, 2016) and modification of the river channel (AMS pers. obs.). The aim of this study was to determine the magnitude of the January 2012 flood relative to previous floods in the headwaters of the Klaserie River catchment and attempt to identify rainfall patterns that resulted in large floods in the perennial headwaters of a lowveld river.

STUDY SITES AND METHODS

The Klaserie River, a minor tributary of the Olifants River (Limpopo River System) in the lowveld region of South Africa, drains the north eastern escarpment of South Africa and confluences with the Olifants River in the Kruger National Park (Fig. 1). From the source (elevation 1600 m) to the Olifants River confluence (elevation 275 m) the 120 km long river drains a catchment area of 852 km^2, mostly subtropical savanna. The Klaserie Catchment is divided into two quaternary sub-catchments; the upper Klaserie River above Klaserie Dam, formerly Jan Wasserman Dam, and the lower Klaserie River between Klaserie Dam and the confluence with the Olifants River. Only the upper Klaserie was included for this study.

The topography of the upper Klaserie River is complex and associated with meso-scale atmospheric circulation and different climatic zones (Pretorius and Rautenbach, 2012). The sub-catchment falls within the Cwa Köppen-Geiger climate classification; humid sub-tropical with dry winter and hot summer (Peel *et al.*, 2007). Mean daily temperature is between 18 and 28°C in summer and 10 and 22°C in winter, while the annual temperature ranges between 5 and 35°C. Rainfall increases with increasing elevation. The Mariepskop area at the top of the catchment has a very wet climate, with rainfall averaging about 2500 mm per annum. The wettest months are December, January and February with monthly rainfall means of 205, 245, and 286 mm respectively, while June, July and August are the driest months with monthly rainfall means of 23, 19, and 21 mm respectively (Van der Schijff and Schoonraad, 1971). Heavy downpours of 50 mm or more within 24 hours are not unusual and mist is frequent (Van der Schijff and Schoonraad, 1971). The lower reaches of the catchment receive less than 500 mm per annum, with February being the wettest month receiving an average rainfall of 118 mm and July the driest month with an average rainfall of 5 mm (Klaserie Private Nature Reserve, *unpublished*).

The upper Klaserie River sub-catchment falls entirely within the Southern Temperate Highveld aquatic ecoregion (Abell *et al.*, 2008). Igneous and metamorphic rocks dominate the basement geology, predominantly Swazian Potassic and Nelspruit suite granite/gneiss (Johnson *et al.*, 2006). The remainder of the basement geology are sedimentary rocks from the Wolkberg Group of the Transvaal Supergroup. The soils of the upper Klaserie sub-catchment are predominantly chromic luvisols and orthic acrisols (FAO, 1995).

Three vegetation biomes are represented in the upper

Klaserie sub-catchment: forest, grassland and savanna (Mucina and Rutherford, 2006). The savanna biome makes up more than 75% of the sub-catchment area, with 18% forests and 5% grasslands. The upper Klaserie River is relatively pristine with more than 70% of the sub-catchment area considered to be in a natural state. There are limited anthropogenic impacts on water quality above human settlements which border a short stretch of the river in the lower part of the sub-catchment. The land cover at higher altitudes is mostly forest; Northern Mistbelt Forest (Mucina and Rutherford, 2006), but this has been reduced through afforestation. Afforestation began in the 1930's and by the 1960s much of the upper catchment had been converted to *Pinus* and *Eucalyptus* plantations. Forestry currently comprises 20.1 km^2 (Perry, 2014), about 12% of the catchment area. Indigenous forest remains in gullies, ravines, and other steep slopes. Over the past decade, some plantations have been abandoned and transformed to either secondary grassland, forest, or thickets. The lower altitudes of the sub-catchment contain limited rural residential areas (about 10% of the sub-catchment area) and dryland subsistence agriculture and fallow lands (about 3% of the sub-catchment area). Numerous wetlands occur in the catchment, with at least one known to have been physically altered through partial drainage.

Historical data

Historical river flow time series data were acquired from the Department of Water and Sanitation's Resource Quality Services web site (Department of Water and Sanitation, 2021) for the gauging stations at the Klaserie Dam wall (B7R001) and the Fleur-de-Lys weir (B7H004). Daily rainfall data from 1960 to 2021 were sourced from two weather stations; Mariepskop forestry station (E 030.86900°; S 24.58476°, altitude of 1315 m asl) and Salique forestry station (E 030.90904°; S 24.60679°, altitude of 930 m asl) (Fig. 1).

Statistical analyses

All maps, graphs and statistical analyses were gener-

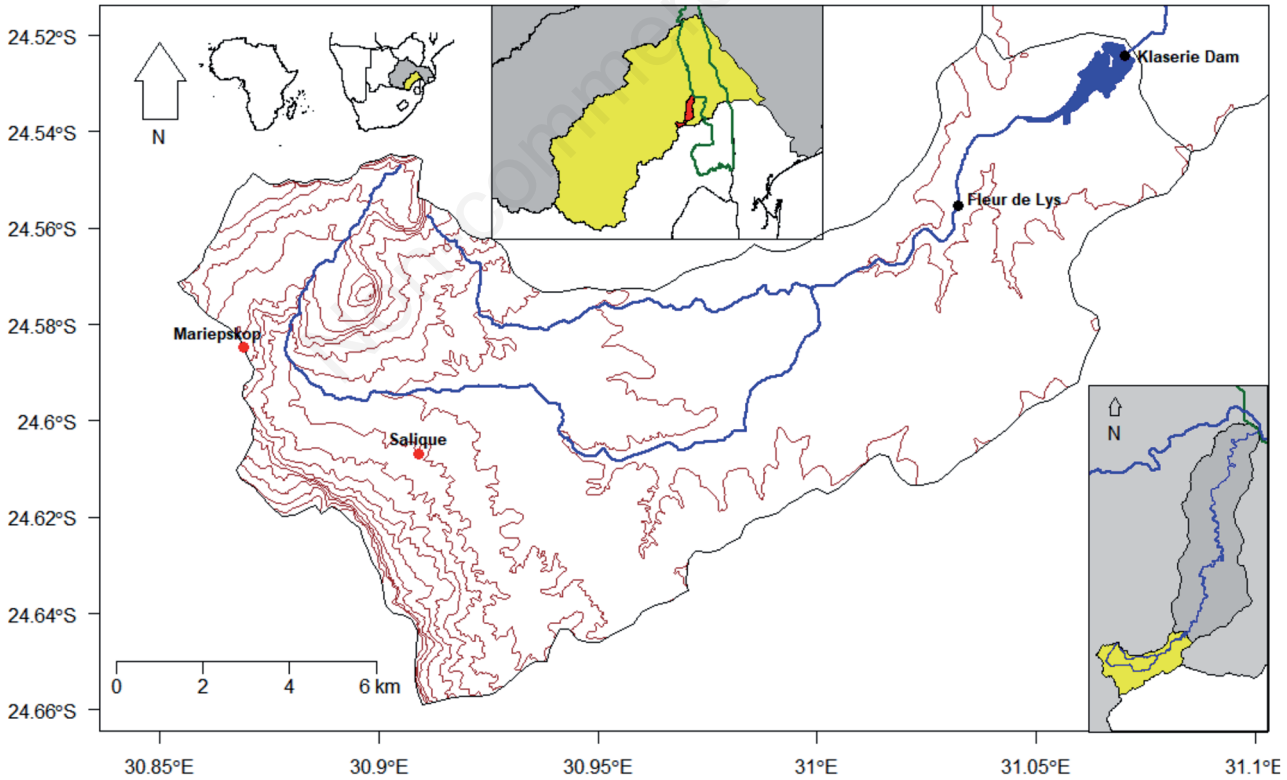

Fig. 1. Map of the upper Klaserie River catchment showing locations of the Fleur de Lys (B7H004) and Klaserie Dam (B7R001) gauging stations and Mariepskop and Salique weather stations. The upper Klaserie River is shown in relation to the Klaserie River catchment (inset), the Olifants River (red area within the yellow area representing the Olifants River catchment, and regionally in relation to the Limpopo River System, indicates by the grey area.

ated/performed using the R 4.2.2 statistical software (R Development Core Team, 2022). Results were considered statistically significant at $p<0.05$.

Catchment geomorphology

The basic catchment parameters, including catchment area (A), catchment perimeter (P), length of the basin along the main stem (L), total length of all streams (Lu), number of streams by stream order (nu) *sensu* Strahler (1957), and maximum and minimum elevations (ELEVmax and ELEVmin, respectively) were compiled using QGIS (https://www.qgis.org/en/site/). The geomorphological parameters of a catchment can be grouped into three main categories: catchment geometry (*e.g.*, form factor, elongation ratio, circularity ratio), drainage network (*e.g.*, bifurcation ratio, drainage density, stream frequency, texture ratio) and relief characteristics (*e.g.,* basin relief, relief ratio, ruggedness number) compiled from Horton (1945), Miller (1953), Schumm (1956) Strahler (1957), (Gardiner and Park, 1978), Goudie *et al.* (2003), Goudie (2004), and Chopra *et al.* (2005). The geomorphological parameters calculated for the upper Klaserie River catchment are summarised in Tab. 1. In addition, linear regressions of the log of the number of streams in each stream order as a function of the stream order was performed using the *lm* function in R. The bifurcation ration (Horton, 1945) was then calculated as the antilog of the slope of the regression. Similarly, the length ratio (Horton, 1945) was calculated from the regression of the log of total length of stream in each stream order as a function of the stream order.

Rainfall data

Daily rainfall data from 1960 to 2021 from both forestry stations were summed for each year. Linear regression was used to compare the annual and daily rainfall records from the two forestry stations using the *lm* function in R. A modified *t*-test was used to test whether the slopes of the linear regressions were statistically different from 1 following Hannweg *et al.* (2020); see Supplementary Material for R code. A significant result for the modified t-test indicates that the slope differs significantly from a 1:1 relationship between the rainfall recorded at the two forestry stations.

The monthly mean, standard deviation, and coefficient of variation were calculated for the mean daily flows at the Fleur-de-Lys gauging station and rainfall data from the Mariepskop forestry station for 1960 to 2021. These were plotted to explore variations in runoff and rainfall over the year and identify the hydrological year for the sub-catchment.

To explore whether any changes between the frequencies of these rainfall events could be detected over the study period, 1960 to 2021, the number of days with rainfall greater than 50, 75, 100 and 150 mm were tallied for each hydrological year grouped into 5- and 10-year periods. Shapiro-Wilk tests (*shapiro.test*) indicated non-normal distributions ($p<0.001$) for both 5- and 10-year periods. Therefore, non-parametric Kruskal-Wallis tests were performed (*kruskal.test*) to determine whether there were significant differences in the frequency of the specified rainfall events. Prior to the Kruskal-Wallis test, the Ljung-Box test was conducted to determine whether the residuals of the time series were independently distributed, to confirm data were not autocorrelated, using the

Tab. 1. Formulae for the calculation of geomorphological parameters for the Upper Klaserie River sub-catchment expressed in terms of catchment area (A), catchment perimeter (P), length of the basin along the main stream (L), total channel length in the catchment (L_c), the number of streams with Strahler stream order u (N_u), and the maximin and minimum elevations in the catchment ($ELEV_{max}$ and $ELEV_{min}$, respectively).

Geomorphological parameter	Formula
Shape factor	$S = \frac{L^2}{A}$
Circulatory ratio	$R_c = \frac{4\pi A}{P^2}$
Form factor	$R_f = \frac{A}{L^2}$
Elongation ratio	$R_e = \sqrt{\frac{A}{4\pi L^2}}$
Bifurcation ratio	$B_r = \frac{N_u}{N_{u+1}}$
Drainage density	$D_d = \frac{L_c}{A}$
Constant of channel maintenance	$C_c = \frac{1}{D_d}$
Stream frequency	$S_f = \frac{N}{A}$
Drainage texture	$D_t = \frac{N}{P}$
Infiltration number	$I_r = D_d * S_f$
Length of overland flow	$L_f = \frac{0.5}{D_d}$
Basin relief	$R_b = ELEV_{max} - ELEV_{min}$
Relief ratio	$R_r = \frac{R_b}{L}$
Ruggedness number	$R_n = D_d * R_b$

Box.test function in R. The Ljung-Box test was conducted with lags of 1, 5, and 10 years to evaluate whether there was autocorrelation at these intervals. The null hypothesis for the Ljung-Box test is that the residuals are independently distributed and the preferred outcome is failure to reject the null hypothesis, *i.e.*, $p > 0.05$.

Flow data

One rating table, calibrated in 1960, was found for Klaserie Dam, while three rating tables were found for the Fleur-de-Lys gauging station; calibrated in 1950, 1986, and 2002. The 1950 and 1986 rating curves were calibrated to a stage height of 4.5 m, while the 2002 rating curve was only calibrated to 2.07 m. One flood exceeded the 2002 rating table calibration, reaching a stage height greater than 5 m. A power curve fitted was to the three Fleur-de-Lys rating table's data to allow for estimation of the discharge based on the measured stage height for this period (Supplementary Fig. 1).

The flow data for the entire Fleur-de-Lys data set was recalculated using the measured stage height and the rating curves derived for the respective periods. Time series plots of the daily average flow for the Fleur-de-Lys gauging weir (B7H004) and Klaserie Dam wall (B7R001) were used to identify flood events. Where possible, hydrographs were prepared for selected floods. The mean daily flow was used to calculate the flow duration curves. The mid-point of that mean daily flow class interval (y-axis) were plotted against the cumulative frequency of the daily flow class intervals (x-axis). A flow duration curve was prepared for the Fleur-de-Lys gauging weir for 1950 to 2021, and for the Klaserie Dam gauging station for 1960 to 2021.

Pardé coefficients (Pardé, 1964) were calculated from these monthly run-off values following Trubilowicz *et al.* (2013):

$$Pk_i = \frac{1}{n}\sum_{j=1}^{n}\left(\frac{Q_{ij}}{\left(\frac{1}{12}\sum_{i=1}^{12} Q_{ij}\right)}\right)$$

where Pk_i is the Pardé coefficient for month i, i is the month, j is the year, and Q_{ij} is run-off in month i and year j (m^3s^{-1}). The Pardé coefficient Pk_i represents the ratio of the mean average run-off in month i to mean annual run-off. The Pardé coefficients sum to 12 for each year. The Pardé coefficients were calculated for the entire study period and for each decade included in the study period. Non-Metric Multi-Dimensional Scaling (NMDS) and Cluster Analysis were performed to determine whether there was evidence of changes in the decadal Pardé coefficients using the vegan package for R (Oksanen *et al.*, 2018). Euclidean distance was used to construct a resemblance matrix using the *vegdist* function, while the NMDS and cluster analyses were conducted using the *metaMDS* and *meandist* functions, respectively.

Flood frequency analysis

The global increase in precipitation extremes (Brooks *et al.*, 2020; Fowler *et al.*, 2021) has not resulted in a corresponding increase in flood intensity (Sharma *et al.*, 2018). Rather, an increase in the frequency of floods has been observed (Hirsch and Archfield, 2015). Prediction of the probability of flood events has traditionally been based on flood frequency analysis (Davie and Quinn, 2019) based on the assumption of flow stationarity (Kim *et al.*, 2018; Do *et al.*, 2020), defined by Milly *et al.* (2008) as "*natural systems fluctuating within an unchanging envelope of variability*." However, climate and landscape change predict non-stationarity in rainfall and flood frequencies and the stationarity assumption of traditional flood frequency may no longer be applicable (Milly *et al.*, 2008; Villarini *et al.*, 2018). Non-stationarity can be manifest as periodicity, a trend, or step change in the mean and/or variance of time series data (Slater *et al.*, 2021b).

The peaks over threshold (POT) approach with a generalized Pareto distribution was used to compile flood series because it is more robust under non-stationary conditions than traditional methods using Gumbel and log-Pearson Type III distributions (Khaliq *et al.*, 2006). Two important considerations of POT analysis are the determination of the threshold level and validation that the exceedances are independent, and not associated with the same flood event (Mostofi Zadeh *et al.*, 2019). The threshold level was chosen using the semi-automated process recommended by Durocher *et al.* (2018) based on the mean residual life, dispersion index, and threshold choice plots, generated using the POT package for R (Ribatet and Dutang, 2022). To reduce the risk of dependent observations, the exceedances were declustered by removing exceedances separated by less than a minimum time span using the *cluster* function of the POT package. Selecting the maximum value in each cluster helps in achieving the needed statistical independence among the POT observations (Mostofi Zadeh *et al.*, 2019). Because the floods in the upper Klaserie River were mostly of short duration, the minimum value for each cluster was set to 3 days. Once the threshold had been chosen, the exceedance events were extracted and declustered. A generalised Pareto distribution was generated using the *fitgpd* function of the POT package using maximum likelihood estimation. A return level plot was then generated for the upper Klaserie River and the estimated magnitude of 5-, 10-, 20-, 50-, 100- and 200-year floods were calculated. The estimated return period for the January 2012 flood was then calculated.

Predictors for floods

To explore whether floods at Fleur-de-Lys gauging station could be predicted from rainfall, the day-to-day change in mean daily flow was used as the dependent variable. To

focus on substantial increases in mean daily flow, and to reduce the extent of the dataset, a minimum increase in mean daily flow of 0.5 m^3s^{-1} was selected. This threshold was selected as the mean daily flow was less than this for over 60% of the days in the dataset. Cumulative rainfall for periods of 2, 3, 7, 14, and 28 days (ending on the day of interest) were calculated and used as an independent variable, in addition to the rainfall for the day, and mean daily flow for the previous day. The rainfall variables were calculated for both the Mariepskop and Salique forestry stations data and analysed separately. Since the aim was to determine whether there was a link between the rainfall and increases in flow, records where the two-day cumulative rainfall less than 50 mm for an increase in mean daily flow were excluded. Regression trees were used to identify conditions that resulted in increases in mean daily flow exceeding 0.5 m^3s^{-1} using *rpart*; rpart package (Therneau *et al.*, 2013). To provide context, the positions of the top 5 increases in mean daily flow, all exceeding 45 m^3s^{-1}, within the decision tree were noted.

RESULTS

For the gauging station at Fleur de Lys, primary data were available from 01/11/1950 to 19/04/2021, although there were gaps in the records, the most significant being between 01/09/1999 and 01/01/2004 while the Fleur-de-Lys gauging station was being rebuilt. The average annual frequency of the daily records prior to 01/09/1999 was 2.2 records per day. From 2004, the average annual frequency of the daily records was 87.5 records per day, reaching a maximum 120 records per day at times (Supplementary Fig. 2). The difference in the temporal resolutions of data complicated comparison between floods that occurred prior to 2000 and floods after 2004. For the Klaserie Dam, records were available from 01/09/1961 to 31/03/2021. The average annual frequency of the daily records prior to 2005 was 0.63 records per day and 30.29 thereafter (Supplementary Fig. 2).

Catchment geomorphology

The geomorphological parameters for the upper Klaserie River sub-catchment are summarised in Tab. 2. The sub-catchment has an area of 164 km^2 with a dendritic drainage pattern. The main stem of the Klaserie River flows 33 km long with an elevational change of 1160 m, a basin relief of 0.035. The ruggedness number of 2.72 lies towards the upper limit of the 2.0 or 3.0 range for a first or second-order basin (Goudie, 2004). The Klaserie River is a 5th order stream at both Fleur de Lys and Klaserie Dam gauging stations.

Rainfall and flow

The annual rainfall recorded at the Mariepskop forestry station was consistently greater than that of the Salique forestry station (regression slope=0.727; adjusted R^2=0.684) and the regression slope differed significantly from 1 (modified *t*-test p<0.001). Similarly, the monthly rainfall at the Mariepskop forestry station was consistently greater than that of the Salique forestry station (regression slope=0.603) and the regression slope differed significantly from 1 (modified *t*-test p<0.001), however, this regression line was a poor representation of the data because it described less than 40% of the variation within the data (adjusted R^2=0.367). The increased rainfall at Mariepskop may be due to increased orographic precipitation because the Mariepskop station is on the watershed between the Kalserie and Blyde river catchments and almost 400 m higher than the Salique station (Supplementary Fig. 3).

The rainfall and mean daily flow relationship for the upper Klaserie catchment followed a hydrological year commencing between May and September (Fig. 2a). Rainfall generally peaked in January, while the mean daily flow peaked in February. The mean daily flow was considerably higher from February to May than from August to November despite similar monthly rainfall totals. This was likely due to infiltration of rain water into the ground water increasing soil saturation from August to January and draining of the ground water from February to May, see Wasko *et al.* (2020). The coefficient of variation for the mean daily flow was greater than 100% throughout the year (Fig. 2b), a characteristic of South African rivers (Davies and Day, 1998). For rainfall, the coefficient of variation was between 50 and 85% for the wet months, October to April, increasing to 160% for the dry months, June to September (Fig. 2b).

The Ljung-Box test failed to reject the null hypothesis that the residuals in the annual rainfall for the Mariepskop forestry station by year, 5-years and decade were independently distributed (all p>0.7). Comparison of the annual rainfall over 5- and 10-year periods found no significant differences (Supplementary Tab. 1). Similarly, no significant differences were found between the frequencies of rainfall events greater than 50, 75, 100 and 150 mm for both the 5- and 10-year periods (Supplementary Tab. 1).

Flow duration curves

For Fleur-de-Lys, the largest flood occurred in January 2012, followed by January 1976, March 1972, March 1956, and February 2021 floods (Fig. 3a). The flow at the Klaserie Dam wall confirmed that the January 2012 flood being the largest, followed by the March 1993, January 1976, and February 2000 floods (Fig. 3b). No flow data were available for the February 2000 flood for Fleur-de-Lys.

Flow duration curves based on mean daily flows are shown in Fig. 4. For Fleur-de-Lys, there was flow almost constantly throughout the evaluation period, and the curve is typical of a perennial headwater stream with no regulation. The Klaserie Dam wall only spilled about 35% of the time and, since this dam has no sluices, it only discharges downstream when spilling.

Tab. 2. Summary of geomorphological parameters for the Upper Klaserie River sub-catchment.

Geomorphological parameter	Calculated value				
Area	164.46 km^2				
Perimeter	72.45 km				
Catchment length along main stem	32.70 km				
Total stream length in the catchment	386.34 km				
Strahler stream Order	1	2	3	4	5
Number of streams by Strahler order	320	74	17	4	1
Total length of streams by Strahler order	220.7	79.5	45.6	21.1	19.4
Mean length of streams by Strahler order	0.69	1.07	2.68	5.27	19.42
$ELEV_{max}$	1700 m				
$ELEV_{min}$	540 m				
Shape factor	6.502				
Circulatory ratio	0.247				
Form factor	0.154				
Elongation ratio	0.111				
Strahler stream orders	1:2	2:3	3:4	4:5	
Length ratio	2.775	1.746	2.166	1.085	
Bifurcation ratio	4.324	4.352	4.250	4.000	
Bifurcation ratio (regression)	4.244				
Length ratio (regression)	1.857				
Drainage density	2.349 km^{-1}				
Constant of channel maintenance	0.426 km				
Stream frequency	2.541 km^{-2}				
Drainage texture	5.770 km^{-1}				
Infiltration number	5.971 km^{-1}				
Length of overland flow	0.213 km				
Basin relief	1160 m				
Relief ratio	0.036				
Ruggedness number	2.725				

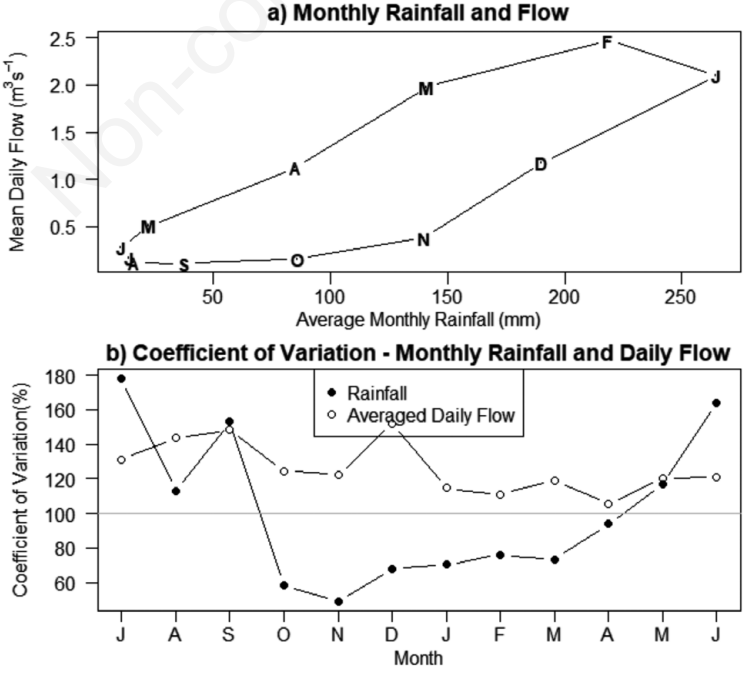

Fig. 2. a) The relationship between monthly rainfall in the upper Klaserie catchment (Mariepskop station) and averaged daily flow at the Fleur-de-Lys gauging station and b) the coefficient of variation for monthly rainfall and averaged daily flow.

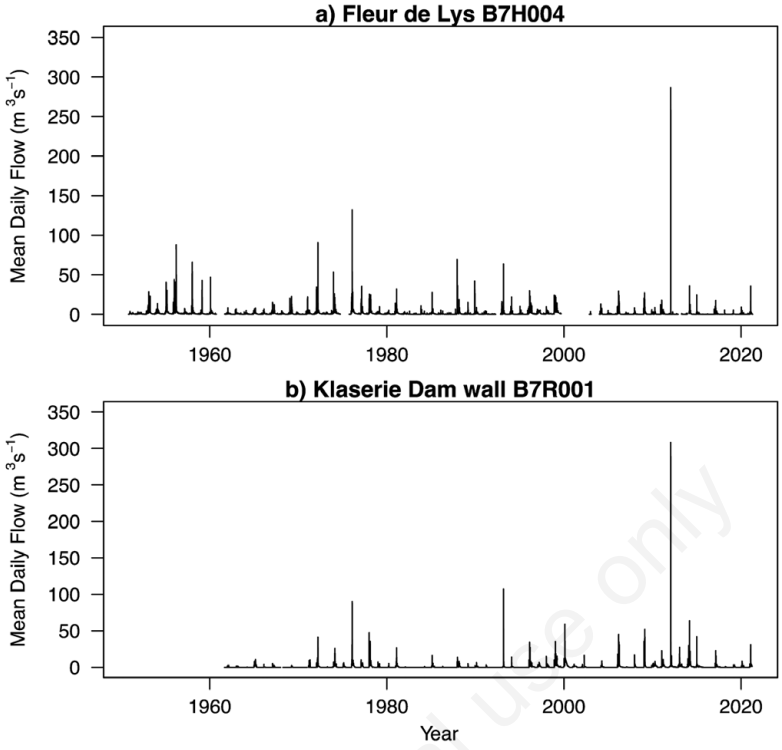

Fig. 3. Mean daily flow for a) the Fleur-de-Lys gauging station (B7H004) and b) Klaserie Dam wall gauging station (B7R001).

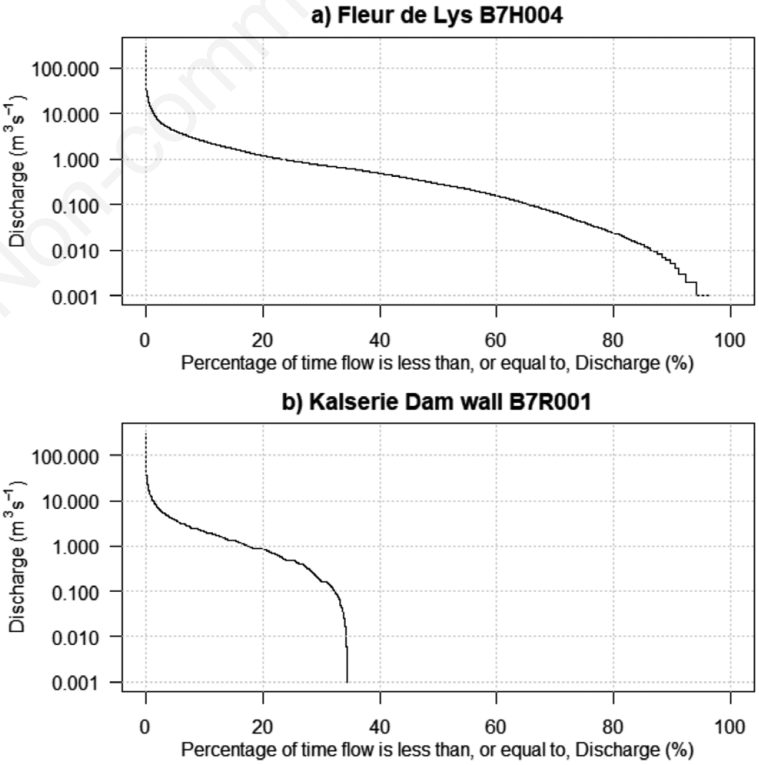

Fig. 4. Revised mean daily discharge and flow duration curve for a) the Fleur-de-Lys gauging station (B7H004), and b) the Klaserie Dam wall gauging station (B7R001) on the upper Klaserie River.

The mean and decadal Pardé coefficients calculated for the Klaserie River at the Fleur de Lys gauging station show that the flow is greatest from December to March, peaking in February (Tab. 3, Fig. 5a). From the multivariate analyses, there is evidence that the Pardé coefficients for the 1970s and the 1990s are very similar to the mean

Tab. 3. Mean and decadal monthly Parde coefficients for the Upper Klaserie River sub-catchment at Fleur de Lys gauging station (B7H004) from 1950 to 2019.

Month	Mean	1950s	1960s	1970s	1980s	1990s	2000s	2010s
July	0.395	0.372	0.446	0.54	0.569	0.392	0.124	0.253
August	0.265	0.291	0.307	0.377	0.343	0.28	0.053	0.141
September	0.247	0.299	0.196	0.313	0.211	0.223	0.036	0.421
October	0.291	0.309	0.415	0.366	0.331	0.293	0.052	0.175
November	0.538	0.491	0.852	0.48	0.823	0.453	0.473	0.236
December	1.322	1.042	1.403	0.925	1.793	1.413	2.15	0.788
January	2.108	1.972	1.696	2.146	1.25	1.991	2.85	3.011
February	2.645	3.124	2.379	2.265	2.683	2.367	2.152	3.029
March	2.037	1.855	1.879	2.276	1.94	2.415	1.901	2.161
April	1.322	1.149	1.456	1.337	1.254	1.243	1.794	1.272
May	0.54	0.677	0.582	0.593	0.528	0.648	0.337	0.375
June	0.29	0.418	0.387	0.382	0.274	0.281	0.078	0.139

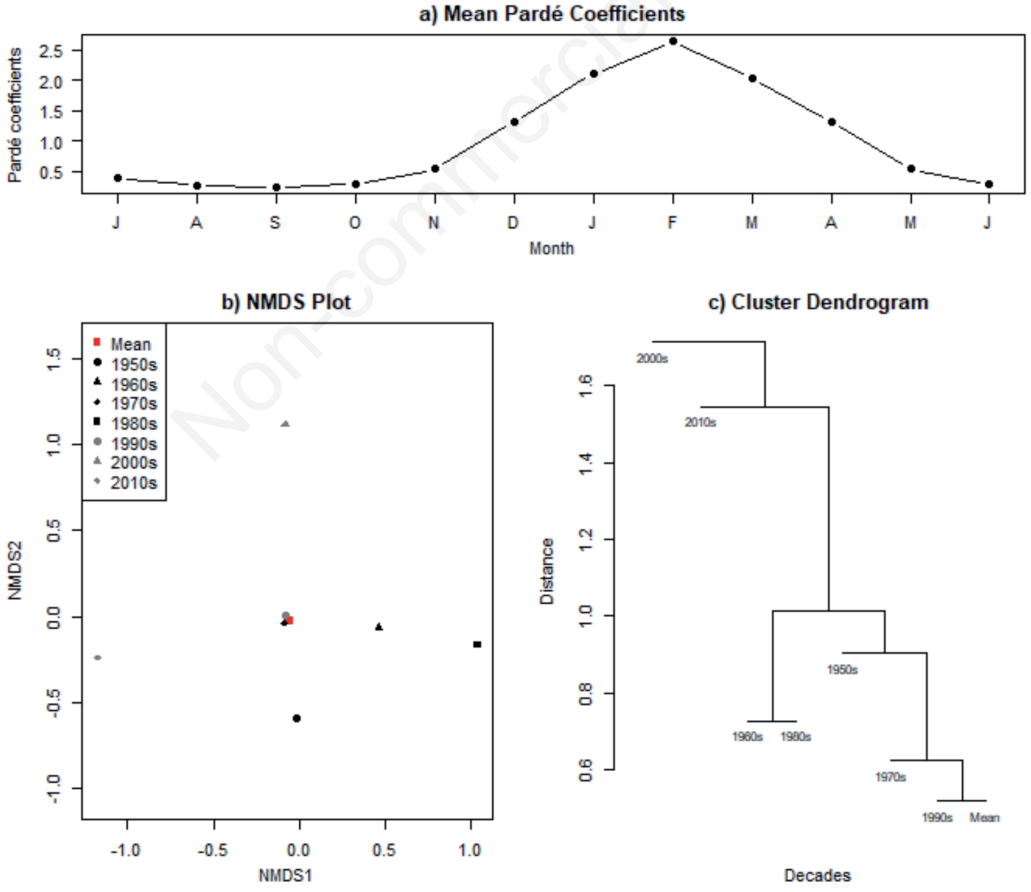

Fig. 5. Multivariate analysis of the Pardé coefficients for the upper Klaserie River at the Fleur-de-Lys gauging station (B7H004) calculated for the entire study period and for decades within the study period: a) mean Pardé coefficients (1950-2019); b) non-metric multi-dimensional scaling plot; c) cluster dendrogram.

Pardé coefficient for the 60 years of the study, while those for the 2000s and 2010s differ considerably to the study period mean (Fig. 5 b,c). Because a single value for the Pardé coefficients was calculated for each decade, it was not possible to determine whether this difference was statistically significant.

Flood frequency analysis

The flood frequency analysis was conducted using 6 m^3s^{-1} as a threshold. The general Pareto distribution fitted to the declustered exceedance data had a scale value of 8.709 (±1.263) and a shape value of 0.429 (±0.125). The density plot shows that the majority of the flows above the threshold are below 50 m^3s^{-1} (Fig. 6a). The predicted flow for floods by the return level are plotted in Fig. 6b and presented for selected return levels in Tab. 4. The predicted return level for the January 2012 flood was calculated to be 225.42 years.

Flood hydrographs

Hydrographs for the January 2012, January 1976, December 1987, and March 1997 floods are presented in Fig. 7. The spill flow from the Klaserie Dam gauging station for the 1976 flood does not correspond to the flow data from the Fleur-de-Lys gauging station. For the 1987 flood, the Klaserie Dam level was more than 4 m below the spillway prior to the flood and the flood peak was contained in the reservoir, therefore, a substantial flood

Tab. 4. Estimated flow for the Upper Klaserie River sub-catchment at Fleur de Lys gauging station (B7H004) at selected return periods.

Return period (years)	Flow (m^3s^{-1})	95% CI (m^3s^{-1})
5	44.43	35.50 – 60.28
10	64.77	50.08 – 99.62
20	92.15	64.65 – 163.74
50	143.40	90.903 – 316.56
100	198.01	*
200	271.52	*

**Confidence interval calculation could not be completed because a value of infinity was returned in the intermediate results.*

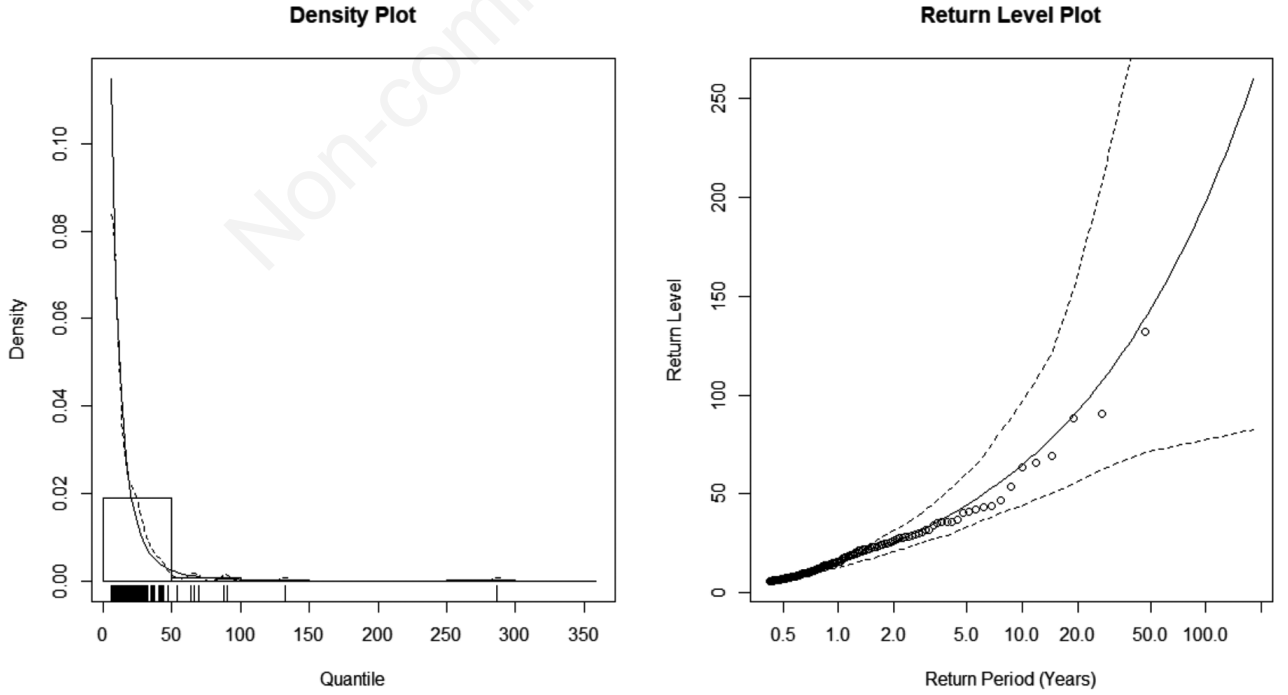

Fig. 6. Density and return level plots for flood discharges for the Fleur-de-Lys gauging station (B7H004) on the upper Klaserie River for the period November 1950 to April 2021 generated using the peaks over threshold method to construct a generalised Pareto distribution for extreme events.

peak was not recorded at the Klaserie Dam wall (Supplementary Fig. 4). For the 2012 flood, the estimated flood peak of 1200 m^3s^{-1} at Fleur-de-Lys gauging station corresponded to the 800 m^3s^{-1} flood peak at the Klaserie Dam wall.

Predictors for floods

For the regression tree analyses, 286 and 261 records of increases in mean daily flow greater than 0.5 m^3s^{-1} were found for the Mariepskop and Salique rainfall data. For Mariepskop, the regression tree had four terminal groups (Fig. 8a). The top 5 flow increases were distributed between the two groups with the highest mean increase in daily flow. The first group had a mean increase in daily flow of 71.1 m^3s^{-1} and was delineated by a two-day cumulative rainfall greater than 240.2 mm. Four of the top 5 flow increases were contained in the eight records for this group. The final top 5 flow increase was in the group with an average increase in daily flow of 23.7 m^3s^{-1}, which was delineated by a two-day cumulative rainfall less than 240.2 mm, mean daily flow greater than 3.2 m^3s^{-1} on the day before the increase, and a 28-day rainfall exceeding 678 mm. For Salique, the regression tree again had four terminal groups, Fig. 8b. The top 5 flow increases were again distributed between the two groups with the highest mean increase in daily flow. The first group had had average increase in daily flow of 71.4 m^3s^{-1} and was delineated by a two-day cumulative rainfall greater than 211.7 mm. Four of the top 5 were contained in the eight records for this group. The final top 5 flow increase record was in the group with an average increase in daily flow of 12.1 m^3s^{-1}, which was delineated a two-day rainfall less than 211.7 mm, a 28-day rainfall greater than 341.9 mm.

Four of the top 5 flow increases (January 2012, January 1976, December 1987, and February 1960) were common to the first groups of the Mariepskop and Salique regression trees, which were delineated by two-day cumulative rainfall figures. The remaining record of the top 5, March 1972, is an anomaly because it has 14-day cumulative rainfall figures of 138 and 141 mm for the Mariepskop and Salique weather stations, respectively, without any discernible short-term rainfall association for the increase in mean daily flow. When the criteria for the first groups of the Mariepskop and Salique data were applied to the full rainfall record, only the aforementioned four records were common. None of the records where no flow data were available for the Fleur-de-Lys gauging station met both criteria.

DISCUSSION

Five major floods have occurred in the upper Klaserie river over the past 50 years, of which the 2012 flood was by far the largest. The 2012 flood caused substantial economic damage (Fitchett *et al.*, 2016) and modification of the river channel (AMS, *personal observation*). Flows in excess of 1200 m^3s^{-1} were recorded at the peak of this flood in a stream with an average flow less than 1 m^3s^{-1}. The upper Klaserie is restricted to a single channel for most of

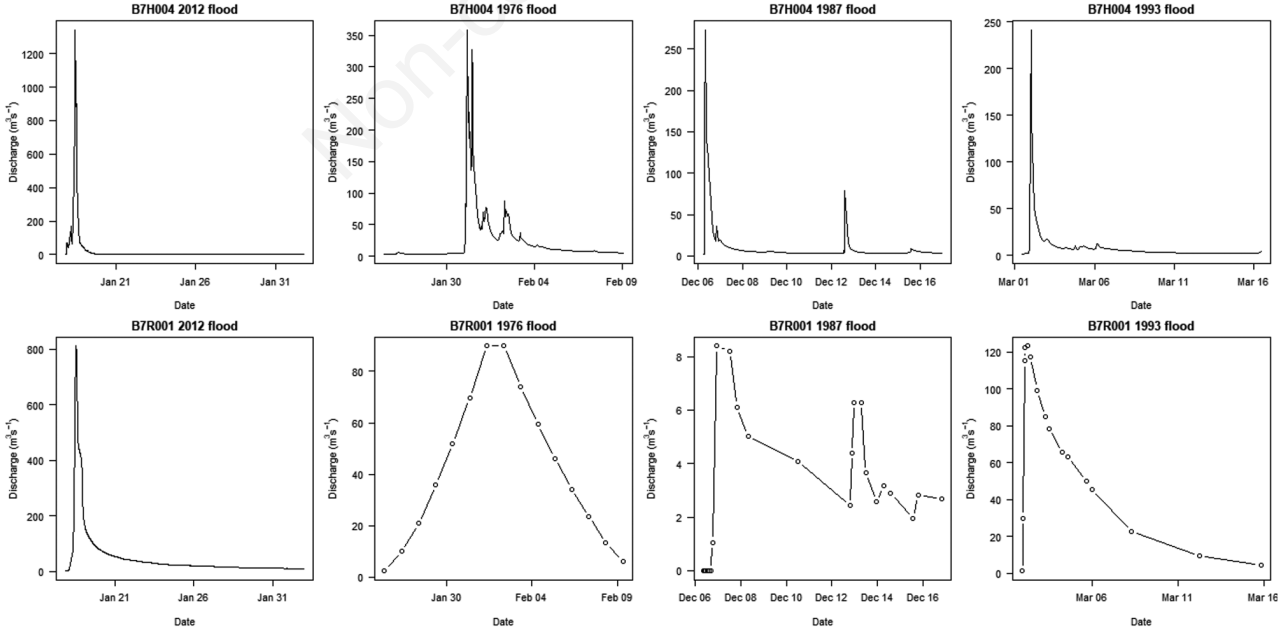

Fig. 7. Hydrographs for the four largest floods recorded at the Fleur-de-Lys (B7H004) and Klaserie Dam (B7R001) gauging stations on the Klaserie River.

the study area but becomes anastomosing below the Fleur de Lys gauging station. For the majority of the study area, the substrate consists of bedrock overlain with boulders, cobbles, gravel and sand. The high water velocities resulted in the finer sand and gravel substrate being reduced in the upper reaches of the study area and consolidation of the anastomosing reaches into fewer channels below Fleur de Lys (SAEON, unpublished data). There was also a substantial removal of trees and shrubs in the anastomosing reaches. An increase in the frequency of moderate to large floods in the lowveld predicted from climate change could result in the frequent stripping of in channel vegetation communities from the anastomosing reaches of the Klaserie River as observed for the Olifants and Sabie rivers in the Kruger National Park communities (Parsons *et al.*, 2005; Milan *et al.*, 2018).

Flood frequency analysis indicated that the 2012 flood exceeded the magnitude predicted for a 1-in-100-year flood with an estimated return frequency of 225 years. Based on the classification of Nathan and Weinmann (2019), floods with return levels between 20 and 100 years are considered to be moderate and rare while floods return levels between 100 and 1000 years are considered to be large and very rare. However, it should be noted that the wet season data were not complete for about 12 of the years covered by this study and that additional large floods could have occurred in these periods, particular in 2000. Considering that climate change models predict an increase in frequencies of severe rainfall events (de Wit and Stankiewicz, 2006) and sub-tropical cyclones making landfall in southern Africa (Fitchett, 2018), the frequency of floods of this magnitude is likely to increase. Our analysis of 5- and 10-year rainfall periods was inconclusive and could not identify significant shifts in the frequency of daily rainfall events greater than 50, 75, 100 and 150 mm. However, the large coefficient of variation for annual and monthly rainfall makes it difficult to discern long-term trends in rainfall based on the 60 years of data analysed. Furthermore, our trend analysis was based on data from a single weather station. A significant difference was found for the rainfall between the two weather stations, which were 5.25 km apart and had an elevation difference about 400 m. The lower elevation Salique weather station reported an almost 25% lower annual rainfall than the higher elevation Mariepskop station. This suggests substantial spatial variation of rainfall within the upper Klaserie River.

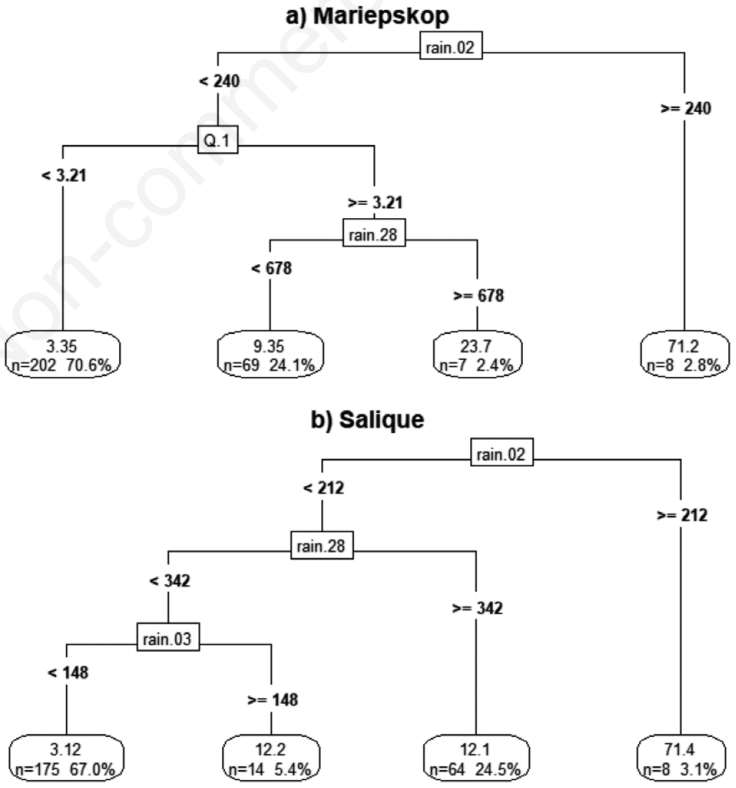

Fig. 8. Regression trees describing the relationship between cumulative rainfall and the increase in the mean daily flow at the Fleur-de-Lys gauging station (B7H004) based on rainfall data from a) the Mariepskop and b) the Salique weather stations. Numbers at the end of each branch show the increase in mean daily flow, 'Q.1' is the mean daily flow on the day before the increase and 'rain.xx' represents the cumulative rainfall for xx days including the day of the increase.

The regression tree analysis provided some insights regarding the rainfall drivers of the extreme floods recorded. Four of the five largest increases in mean daily flow at the Fleur-de-Lys occurred when the two-day cumulative rainfall recorded at the Mariepskop and Salique weather stations exceeded 240 mm and 212 mm, respectively. For the 2012 flood, this value exceeded 400 mm at both weather stations. However, the March 1972 flood, the third largest flood on record, did not meet either of the aforementioned criteria and had comparatively low 14-day cumulative rainfall at both weather stations. It was not possible to determine whether this is an artefact of the rainfall or flow records. When the regression tree criteria were applied to the rainfall data over periods where there was no flow data available for Fleur-de-Lys, there were periods where the criterion of one weather station was met, but not both. In most of these cases, there was considerable disparity between the cumulative rainfall figures from the two weather stations. For example, from the 18th to 20th of February 2001, 1400 mm of rainfall was reported for the Salique weather station, however, only 222 mm rainfall was recorded at the Mariepskop; for the 21st of December 2001 the two-day cumulative rainfall at Mariepskop was 400 mm but the 14-day cumulative rainfall figure for Salique was only 41 mm; and on the 19th of March 2000 the two-day cumulative rainfall at Mariepskop was 387 mm but the 14-day cumulative rainfall figure for Salique was only 229 mm. These examples all occurred over a period between 1999 and 2004 when the Fleur-de-Lys gauging station was being rebuilt. Unfortunately, the spillage data for the Klaserie Dam gauging station is also incomplete over this period. Intense Tropical Cyclone Leon-Eline, which made landfall in Mozambique on the 22nd of February 2000, caused severe flooding in the Limpopo and Nkomati-Crocodile River systems, including the Olifants River. However, the rainfall recorded at both weather stations was only 100 mm for the 23 of February 2000. Tropical storms or cyclones moving over the region that resulted in similar floods events were Very Intense Tropical Cyclone Terry-Danae in January 1976, Tropical Cyclone Eloise in January 1987 and Subtropical Depression Dando in January 2012.

Alternatives to the regression tree approach used in this study involve the development of a hydrological model for the catchment based on the unit hydrograph method (Sherman, 1932) or the soil and water assessment tool (SWAT) (Neitsch *et al.*, 2011) incorporating the CN-curve developed by the Soil Conservation Service of the US Dept. of Agriculture (Cronshey, 1986). Changes in land-use can be related to changes in hydrology through the CN-curve. The unit hydrograph method requires an hourly record of rainfall and flow for gauging stations within a catchment. For the upper Klaserie River, the rainfall data from both weather stations were not available on an hourly basis, while the flow data from Fleur de Lys gauging station were only available following the refurbishment of the gauging station in 2004. Therefore, it was not possible to utilise the unit hydrograph method for the current study. Future studies could use this methodology provided rain gauges capable of recording rainfall on an hourly basis are installed at one, or both, weather stations. Such a gauge has already been installed at the Mariepskop station, and another is planned for Salique.

A hydrological model for the upper Klaserie catchment was developed by Perry (2014) using the SWAT methodology and including a CN-curve. The CN-curve was based on the land-use data of the South African National Biodiversity Institute's 2009 land-cover shape file (South African National Biodiversity Institute, 2008). The model was calibrated based on stream flow data from 1993 to 1999 and evaluated based on data from 2004 to 2010. The following parameters were found to be significant in the global sensitivity analysis of the resultant model; the runoff curve number, soil evaporation compensation coefficient, water capacity of the soil layer, threshold depth of water in the shallow aquifer, groundwater delay time, and groundwater 'revap' coefficient. The performance of the hydrological model was satisfactory for the calibration data, but was less accurate for the test data. This may be due to the test data covering the period after the gauging station had been revamped and a new rating curve being used for the test data. Future research could use this hydrological model with a series of land-cover data to evaluate the change in CN-curve as the land-cover changes, based on land-cover data generated from aerial photographs of the catchment.

The SWAT hydrological model could be used to evaluate whether the extremity of the 2012 flood could be attributed to land cover changes in the preceding decade leading to greater severity flooding despite similar rainfall patterns to previous decades. The majority of the forestry plantations in the catchment above the Fleur-de-Lys were decommissioned around the year 2000, and, by 2012, some plantations had been cleared and transformed to secondary grassland, dense savanna, or young indigenous forest. The remaining plantations have since been abandoned, with many invaded by non-native plant species.

Similar hydrological data to those used for this study are available for other headwater streams in South Africa, thanks to the extensive monitoring programme established by the South African government over the past century. While there are deficiencies in these data, which included significant gaps during periods of high flow, low resolution of prior to 2004, and inconsistencies in the stage depth ranges, our study demonstrates that such data can still be used to detect and characterize major floods, and further our understanding of their causes. Continuation of such monitoring, as well as collocated water quality monitoring,

is vital for river health monitoring and the detection of future extreme floods as climate change progresses.

CONCLUSIONS

The January 2012 flood in the upper Klaserie River was the largest flood recorded for this system and had an estimated return level of 225 years using the peaks over threshold methodology with a generalised Pareto distribution. While there were gaps in the data, *e.g.*, between 1999 and 2004 when the 2000 floods caused significant damage in the Olifants River system, this study demonstrated that analyses of flood frequency and flow duration curves were possible for a small headwater stream in southern Africa. Two-day cumulative rainfall was found to be the best predictor of large floods for this stream, although other factors such as land use change are likely to have contributed, at least for the most recent, and largest, flood. A detailed hydrological model, combined with mapping of land cover change, is needed to confirm this, and to enhance our ability to predict future floods of this magnitude. As our analyses for detecting changes in rainfall and flood patterns were exploratory and we further recommend that non-stationarity analyses be performed for to evaluate whether there is evidence of the impact of climate change on these parameters.

ACKNOWLEDGEMENTS

The research reported here was fully funded by the South African Environmental Observation Network (SAEON). Any opinion, findings, conclusions or recommendations expressed are those of the authors and therefore the funding agencies do not accept any liability for them. The authors would like to thank the three anonymous reviewers for their insightful comments and suggestions that improved the manuscript.

REFERENCES

Abell R, Theime ML, Revenga C, Bryer M, Kottelat M, Bogutskaya N, et al. 2008. Freshwater Ecoregions of the world: a new map of biogeographic units for freshwater biodiversity conservation. BioScience 58:403-414.

Allaire M, 2018. Socio-economic impacts of flooding: A review of the empirical literature. Water Secur 3:18-26.

Balian EV, Segers H, Lévèque C, Martens K, 2008. The Freshwater animal diversity assessment: an overview of the results. Hydrobiologia 595:627-637.

Ball J, Babister M 2019. Catchment simulation for design flood estimation. Book 4 in Australian rainfall and runoff: A guide to flood estimation. Commonwealth of Australia (Geosciences Australia): 86 pp.

Brooks N, Clarke J, Ngaruiya GW, Wangui EE, 2020. African heritage in a changing climate. Azania 55:297-328.

Carpenter SR, Stanley EH, Vander Zanden MJ, 2011. State of the world's freshwater ecosystems: physical, chemical, and biological changes. Annu Rev Environ Resour 36:75-99.

Chopra R, Dhiman RD, Sharma PK, 2005. Morphometric analysis of sub-watersheds in Gurdaspur district, Punjab using remote sensing and GIS techniques. J Indian Soc Remote 33:531-539.

Cronshey R, 1986. Urban hydrology for small watersheds. Technical Release 55. US Dept. of Agriculture, Soil Conservation Service, Engineering Division: 162 pp.

Davie T, Quinn NW. 2019. Fundamentals of hydrology. Routledge.: 221 pp.

Davies BR, Day JA, 1998. Vanishing waters. University of Cape Town Press: 487 pp.

de Wit M, Stankiewicz J, 2006. Changes in surface water supply across Africa with predicted climate change. Science 311:1917-1921.

Department of Water and Sanitation, 2021. Surface water quality for the Olifants River. Water Management Systems, Institute for Water Quality Studies, Department of Water and Sanitation, Pretoria.

Do HX, Mei Y, Gronewold AD, 2020. To what extent are changes in flood magnitude related to changes in precipitation extremes? Geophys Res Lett 47:e2020GL088684.

Doocy S, Daniels A, Murray S, Kirsch TD, 2013. The human impact of floods: a historical review of events 1980-2009 and systematic literature review. PLoS Curr 5:ecurrents.dis.f4deb457904936b07c09daa98ee8171a.

Durocher M, Mostofi Zadeh S, Burn DH, Ashkar F, 2018. Comparison of automatic procedures for selecting flood peaks over threshold based on goodness-of-fit tests. Hydrol Process 32:2874-2887.

FAO, 1995. Digital Soil Map of the World and derived properties (ver. 3.5). FAO Land and Water Digital Media Series #1.

Feeley H, Davis S, Bruen M, Blacklocke S, Kelly-Quinn M, 2012. The impact of a catastrophic storm event on benthic macroinvertebrate communities in upland headwater streams and potential implications for ecological diversity and assessement of ecological status. J Limnol 71:109-318.

Fitchett JM, 2018. Recent emergence of CAT5 tropical cyclones in the South Indian Ocean. S Afr J Sci 114:1-6.

Fitchett JM, Hoogendoorn G, Swemmer AM, 2016. Economic costs of the 2012 floods on tourism in the Mopani District Municipality, South Africa. Trans R Soc South Africa 71:187-194.

Fowler HJ, Ali H, Allan RP, Ban N, Barbero R, Berg P, et al., 2021. Towards advancing scientific knowledge of climate change impacts on short-duration rainfall extremes. Philos Trans R Soc A 379:20190542.

Gardiner V, Park CC, 1978. Drainage basin morphometry: review and assessment. Progress Phys Geogr 2:1-35.

Goudie A, 2004. Encyclopedia of geomorphology. Routledge, London: 1202 pp.

Goudie A, Lewin J, Richards K, Anderson M, Burt T, Whalley B, Worsley P, 2003. Geomorphological techniques. Routledge, London: 592 pp.

Hannweg B, Marr SM, Bloy L, Weyl OLF, 2020. Using action cameras to estimate the abundance of threatened fishes in clear headwater streams. Afr J Aquat Sci 45:372-377.

Heritage G, Entwistle N, Milan D, Tooth S, 2019. Quantifying and contextualising cyclone-driven, extreme flood

magnitudes in bedrock-influenced dryland rivers. Adv Water Resour 123:145-159.

Heritage G, Tooth S, Entwistle N, Milan D, 2015. Long-term flood controls on semi-arid river form: evidence from the Sabie and Olifants rivers, eastern South Africa. Proc Int Assoc Hydrol 367:141-146.

Hirsch RM, Archfield SA, 2015. Not higher but more often. Nat Clim Change 5:198-199.

Horton RE, 1945. Erosional development of streams and their drainage basins; hydrophysical approach to quantitative morphology. Geol Soc Am Bull 56:275-370.

Johnson MR, Anhauesser CR, Thomas RJ [eds.]. 2006. The geology of South Africa. Geological Society of South Africa, Pretoria / Council for Geoscience, Johannesburg: 691 pp.

Khaliq MN, Ouarda TBMJ, Ondo JC, Gachon P, Bobée B, 2006. Frequency analysis of a sequence of dependent and/or non-stationary hydro-meteorological observations: A review. J Hydrol 329:534-552.

Kim SU, Son M, Chung E-S, Yu X, 2018. Effects of non-stationarity on flood frequency analysis: case study of the Cheongmicheon watershed in South Korea. Sustainability 10:1329.

King J, Brown C, Sabet H, 2003. A scenario-based holistic approach to environmental flow assessments for rivers. River Res Appl 19:619-639.

Meyer JL, Strayer DL, Wallace JB, Eggert SL, Helfman GS, Leonard NE, 2007. The contribution of headwater streams to biodiversity in river networks. J Am Water Resour As 43:86-103.

Milan D, Heritage G, Tooth S, Entwistle N, 2018. Morphodynamics of bedrock-influenced dryland rivers during extreme floods: Insights from the Kruger National Park, South Africa. Geol Soc Am Bull 130:1825-1841.

Millennium Ecosystem Assessment, 2005. Ecosystem and human well-being: synthesis. World Resources Institute: 155 pp.

Milly PCD, Betancourt J, Falkenmark M, Hirsch RM, Kundzewicz ZW, Lettenmaier DP, Stouffer RJ, 2008. Stationarity is dead: whither water management? Science 319:573-574.

Mostofi Zadeh S, Durocher M, Burn DH, Ashkar F, 2019. Pooled flood frequency analysis: a comparison based on peaks-over-threshold and annual maximum series. Hydrol Sci J 64:121-136.

Mucina L, Rutherford MC, 2006. The vegetation of South Africa, Lesotho and Swaziland. Strelitzia 19. South African National Biodiversity Institute:. 808 pp.

Naiman RJ, Latterell JJ, Pettit NE, Olden JD, 2008. Flow variability and the biophysical vitality of river systems. C R Geosci 340:629-643.

Nathan R, Weinmann PE, 2019. Estimation of very rare to extreme floods. Book 8 in Australian rainfall and runoff: A guide to flood estimation. Commonwealth of Australia (Geosciences Australia): 120 pp.

Neitsch SL, Arnold JG, Kiniry JR, Williams JR. 2011. Soil and water assessment tool theoretical documentation version 2009, p. 506. Texas Water Resources Institute, College Station, TWRI Report TR-191.

Oksanen J, Blanchet FG, Kindt R, Legendre P, O'Hara RB, Simpson GL, et al., 2018. VEGAN: Community Ecology Package version 2.5-3. Available from: http://R-Forge.R-project.org/projects/vegan/

Pardé M, 1964. [Fleuves et rivières].[Book in French]. Armand Colin, Paris: 224 pp.

Parsons M, McLoughlin CA, Kotschy KA, Rogers KH, Rountree MW, 2005. The effects of extreme floods on the biophysical heterogeneity of river landscapes. Front Ecol Environ 3:487-494.

Peel MC, Finlayson BL, McMahon TA, 2007. Updated world map of the Koppen-Geiger climate classification. Hydrol Earth Syst Sci 4:439-473.

Perry KA. 2014. Application of the SWAT hydrological model in a small, mountainous catchment in South Africa. Unpublished MSc Thesis in Water Resource Management, Faculty of Natural and Agricultural Sciences, University of Pretoria: 79 pp.

Pretorius l, Rautenbach H, 2012. A Long-term synoptic-scale climate study over Mariepskop, Mpumalanga, South Africa. Clean Air J 22:2-6.

R Development Core Team. 2022. R: A Language and Environment for Statistical Computing. R Foundation for Statistical Computing, Vienna

Ribatet M, Dutang C. 2022. POT: Generalized Pareto distribution and peaks over threshold. R package version 1.1-10. Available from: https://CRAN.R-project.org/package=POT

Richardson JS, 2019. Biological diversity in headwater streams. Water 11:366.

Schumm SA, 1956. Evolution of drainage systems and slopes in badlands at Perth Amboy, New Jersey. Geol Soc Am Bull 67:597-646.

Sharma A, Wasko C, Lettenmaier DP, 2018. If precipitation extremes are increasing, why aren't floods? Water Resour Res 54:8545-8551.

Sherman LK, 1932. Streamflow from rainfall by the unit-graph method. Engineering News Record 108:501-505.

Sitterson J, Knightes C, Parmar R, Wolfe K, Avant B, Muche M, 2018. An overview of rainfall-runoff model types. EPA/600/R-17/482, 2017. U.S. Environmental Protection Agency: 30 pp.

Slater L, Villarini G, Archfield S, Faulkner D, Lamb R, Khouakhi A, Yin J, 2021a. Global changes in 20-year, 50-year, and 100-year river floods. Geophys Res Lett 48:e2020GL091824.

Slater LJ, Anderson B, Buechel M, Dadson S, Han S, Harrigan S, et al., 2021b. Nonstationary weather and water extremes: a review of methods for their detection, attribution, and management. Hydrol Earth Syst Sci 25:3897-3935. https://doi.org/10.5194/hess-25-3897-2021.

South African National Biodiversity Institute, 2008. Archived National Land Cover 2009 [vector geospatial dataset]. Biodiversity GIS website.

Strahler AN, 1957. Quantitative analysis of watershed geomorphology. Eos T Am Geophys Un 38:913-920.

Therneau T, Atkinson B, Ripley B. 2013. Rpart: Recursive Partitioning. R Package Version 4.1-3. Available from: http://CRAN.R-project.org/package=rpart

Trubilowicz JW, Moore RD, Buttle JM, 2013. Prediction of stream-flow regime using ecological classification zones. Hydrol Process 27:1935-1944.

Turner MG, Dale VH, 1998. Comparing large, infrequent disturbances: what have we learned? Ecosystems 1:493-496.

Van der Schijff HP, Schoonraad E, 1971. The flora of the Mariepskop complex. Bothalia 10:461-500.

Villarini G, Taylor S, Wobus C, Vogel R, Hecht J, White KD, et al., 2018. Floods and nonstationarity: A review. CWTS 2018-01, U.S. Army Corps of Engineers.

Wasko C, Nathan R, Peel MC, 2020. Changes in antecedent soil moisture modulate flood seasonality in a changing climate. Water Resour Res 56:e2019WR026300.

Westra S, Fowler HJ, Evans JP, Alexander LV, Berg P, Johnson F, et al., 2014. Future changes to the intensity and frequency of short-duration extreme rainfall. Rev Geophysi 52:522-555.

Yamashita Y, Kloeppel BD, Knoepp J, Zausen GL, Jaffé R, 2011. Effects of watershed history on dissolved organic matter characteristics in headwater streams. Ecosystems 14:1110-1122.